pathogens

MDPI

Article

Differential TLR-ERK1/2 Activity Promotes Viral ssRNA and dsRNA Mimic-Induced Dysregulated Immunity in Macrophages

Rakshya Shrestha [1], Paige Marie Johnson [1], Roshan Ghimire [1], Cody John Whitley [1] and Rudragouda Channappanavar [1,2,*]

[1] Department of Veterinary Pathobiology, College of Veterinary Medicine, Oklahoma State University, Stillwater, OK 74078, USA; rakshya.shrestha@okstate.edu (R.S.); paige.m.johnson@okstate.edu (P.M.J.); roshan.ghimire@okstate.edu (R.G.); cody.whitley@okstate.edu (C.J.W.)

[2] Oklahoma Center for Respiratory and Infectious Diseases, Oklahoma State University, Stillwater, OK 74078, USA

* Correspondence: rchanna@okstate.edu; Tel.: +1-405-744-7224

Abstract: RNA virus-induced excessive inflammation and impaired antiviral interferon (IFN-I) responses are associated with severe disease. This innate immune response, also referred to as "dysregulated immunity" is caused by viral single-stranded RNA (ssRNA)- and double-stranded-RNA (dsRNA)-mediated exuberant inflammation and viral protein-induced IFN antagonism. However, key host factors and the underlying mechanism driving viral RNA-mediated dysregulated immunity are poorly defined. Here, using viral ssRNA and dsRNA mimics, which activate toll-like receptor 7 (TLR7) and TLR3, respectively, we evaluated the role of viral RNAs in causing dysregulated immunity. We observed that murine bone marrow-derived macrophages (BMDMs), when stimulated with TLR3 and TLR7 agonists, induced differential inflammatory and antiviral cytokine response. TLR7 activation triggered a robust inflammatory cytokine/chemokine induction compared to TLR3 activation, whereas TLR3 stimulation induced significantly increased IFN/IFN stimulated gene (ISG) response relative to TLR7 activation. To define the mechanistic basis for dysregulated immunity, we examined cell-surface and endosomal TLR levels and downstream mitogen-activated protein kinase (MAPK) and nuclear factor kappa B (NF-kB) activation. We identified significantly higher cell-surface and endosomal TLR7 levels compared to TLR3, which were associated with early and robust MAPK (p-ERK1/2, p-P38, and p-JNK) and NF-kB activation in TLR7-stimulated macrophages. Furthermore, blocking EKR1/2 and NF-kB activity reduced TLR3/7-induced inflammatory cytokine/chemokine levels, whereas only ERK1/2 inhibition enhanced viral RNA mimic-induced IFN/ISG responses. Collectively, our results illustrate that high cell-surface and endosomal TLR7 expression and robust ERK1/2 activation drive viral ssRNA mimic-induced excessive inflammatory and reduced IFN/ISG response and blocking ERK1/2 activity would likely mitigate viral-RNA/TLR-induced dysregulated immunity.

Keywords: SARS-CoV-2; TLRs; ERK1/2; interferon; inflammation; macrophages

Citation: Shrestha, R.; Johnson, P.M.; Ghimire, R.; Whitley, C.J.; Channappanavar, R. Differential TLR-ERK1/2 Activity Promotes Viral ssRNA and dsRNA Mimic-Induced Dysregulated Immunity in Macrophages. *Pathogens* **2024**, *13*, 1033. https://doi.org/10.3390/pathogens13121033

Academic Editor: Jochen Bodem

Received: 3 October 2024
Revised: 13 November 2024
Accepted: 19 November 2024
Published: 23 November 2024

1. Introduction

Emerging and re-emerging RNA viruses pose a significant threat to global public health. As opposed to the only dsRNA virus (rotavirus) infecting humans, several dozens of positive- and negative-sense ssRNA viruses cause disease in humans. Most of these ssRNA viruses, such as influenza viruses, flaviviruses, filoviruses, and coronaviruses SARS-CoV, MERS-CoV, and SARS-CoV-2, have zoonotic sources, and their accidental spillover from animal reservoirs into human population has caused multiple epidemics and pandemics [1–6]. In addition to the viruses currently circulating in humans or periodically spilled over from animal sources, many ssRNA viruses (influenza viruses and novel coronaviruses) with zoonotic potential to infect and cause outbreaks in humans have been identified in bats and several

other animal reservoirs [7–10]. Interestingly, compared to DNA viruses (e.g., herpesviruses, adenoviruses, hepadnavirus, and papillomaviruses), the majority of emerging and re-emerging ssRNA viruses cause acute and often severe disease in humans [11]. The fatal illness caused by these RNA viruses is commonly associated with excessive inflammation and impaired antiviral immunity (dysregulated immunity) [12–14]. Consequently, to better understand severe disease caused by the ssRNA viruses, it is critical to define the virus and host factors that drive excessive inflammation and impair antiviral immunity.

Viruses induce antiviral and inflammatory responses following recognition of viral pathogen-associated molecular patterns (PAMPs) by cognate immune sensors [15–17]. The viral ssRNA genome and replication-intermediate dsRNA are two key PAMPs that elicit antiviral and inflammatory response during ssRNA virus infections [18,19]. Among the two viral RNA molecules, ssRNA is highly abundant, and by some estimates, the ratio of ssRNA to dsRNA is >100 to 1 in an active ssRNA virus replicating cell [20,21]. Following infection, the intracellular ssRNA is sensed by the retinoic acid-inducible gene I (RIG-I) receptor, while dsRNA is detected by both RIG-I and melanoma differentiation-associated protein 5 (MDA-5) [22–24]. In contrast, extracellular viral ssRNA and dsRNA, derived from a lytic infection, are detected by cell surface- and endosomal-located TLR7/8 and TLR3, respectively [25,26]. TLR7/8 utilizes myeloid differentiation primary response 88 (Myd88) and TLR3 signals through TIR-domain-containing adaptor-inducing beta interferon (TRIF) to elicit inflammatory and antiviral responses [27–30]. TLR-Myd88 or TRIF signaling further activates mitogen-activated protein kinase (MAPK) or nuclear factor kappa B (NF-kB) to induce inflammatory mediators and interferon regulatory factors (IRFs) to facilitate IFN/ISG response [31–34]. However, the relative contribution of TLR7 and TLR3 activation and the mechanistic basis for TLR7- and TLR3-induced differential antiviral and inflammatory response are not clearly defined.

RNA virus infection of a cell results in the synthesis of both single-stranded RNA and intermediate double-stranded RNA during viral replication [35,36]. These viral RNAs are key PAMPS that drive robust antiviral and inflammatory responses [37,38]. However, the relative contribution of ssRNA and dsRNA to antiviral and inflammatory response has not been well characterized. Additionally, recent studies have suggested the persistence of viral RNAs following the resolution of infection [39,40]. The persistent viral RNA following SARS-CoV-2 infection is associated with immunoinflammatory conditions leading to post-acute COVID-19 sequelae, also known as long COVID [41–43]. Therefore, identification of host targets and cellular mechanisms driving viral RNA-induced inflammation and suppressed interferon response is essential for moderating inflammation and host protection. Viruses possess multiple structural and non-structural proteins (NSPs) that directly interact with IFN signaling proteins, ISGs, and NF-kB to subvert antiviral responses [44–46]. However, the virus-induced antagonism of IFN/ISG activity without directly interacting with intracellular signaling protein(s) is poorly described. Therefore, the primary objective of this study is to elucidate the role of differential cell-surface and endosomal TLR3/TLR7 expression and downstream ERK1/2 activation in viral RNA-induced dysregulated immunity

In this study, to mimic extracellular viral RNA sensing by cell-surface or endosomal TLR3 and TLR7, we treated murine bone marrow-derived macrophages (BMDMs) with R848 (ssRNA mimic/TLR7 agonist) and Poly I:C (dsRNA mimic/TLR3 agonist). Our results illustrate that viral ssRNA and dsRNA mimics induce differential antiviral and inflammatory cytokine responses, which correspond with cell-surface/endosomal TLR3/TLR7 expression and MAPK and NF-KB activation. We also show that viral RNA mimic-induced robust ERK1/2 activation drives dysregulated immunity. Collectively, our results highlight an under-appreciated role of viral ssRNA- and dsRNA-mediated differential ERK1/2 activation in virus-induced dysregulated immunity and, by extension, severe disease.

2. Materials and Methods

Murine macrophage extraction and stimulation of macrophages: Bone marrow cells extracted from C57BL/6 mice were grown in 12-well plates using RPMI medium supplemented with 10% fetal bovine serum, 1% penicillin-streptomycin, 1% L-glutamine, 1% sodium bicarbonate, 1% sodium pyruvate, and 1% non-essential amino acids and were treated with macrophage colony-stimulating factor (m-MCSF, GenScript, Cat # Z02930-50, 40 ng/mL) for 6–7 days, with media change every three days to differentiate bone marrow cells into mouse bone marrow-derived macrophages (BMDMs).

TLR stimulation and MAPK/NF-kB inhibitor studies: For stimulation studies, a confluent monolayer of primary BMDMs was stimulated with R848 (InvivoGen, San Diego, CA, USA, Catalog #tlrl-r848-5, single-stranded RNA mimic) and Poly I:C (InvivoGen, San Diego, CA, USA, Catalog #tlrl-pic, double-stranded RNA mimic), each treated at 5 or 10 ug/mL for 8 or 24 h. After 8 and 24 h of stimulation, cells in Trizol or cell supernatants were collected to assess the mRNA and protein levels, respectively, of inflammatory cytokines and chemokines and type-I interferons (IFN-Is). Primary mouse BMDMs were treated with pathway-specific inhibitors for inflammatory pathway inhibition studies, each at 5 μM concentration. Specifically, we used inhibitors of ERK1/2 (Trametinib, SelleckChem, Houston, TX, USA, Catalog # S2673), p38 (Losmapimod, Selleckchem, Houston, TX, USA, Catalog #S7215), NF-kB (BAY11-7082, SelleckChem, Houston, TX, USA, Catalog #S2913), and JNK inhibitor (Millipore-Sigma Rockville, MD, USA, Catalog #CAS 129-56-6) 2 h before stimulation with R848 or Poly I:C until sample collection at 8 or 24 h for mRNA or protein levels of antiviral and inflammatory cytokines and chemokines.

Enzyme-linked immunosorbent assay (ELISA): We used sandwich ELISA to quantify cytokine levels. Concentrations of TNF- α (BD Biosciences, San Diego, CA, USA Cat#558534), IL-6 (BD Biosciences, San Diego, CA, USA Cat # 555240), MCP-1 (BD Biosciences, San Diego, CA, USA Cat # 555260), and IFN-β (R&D systems, Minneapolis, MN, USA Cat #DY8234-05) in cell culture supernatants were measured using commercially available BD OptEIA™ or Bio-techne ELISA kits as per manufacturer's instructions. A 96-well high-binding microplate (Corning, Catalog #3361) was coated with capture antibody overnight at 4 °C or room temperature. The next day, plates were blocked for 1 h at room temperature, and 100 μL of samples was added to each ELISA well and incubated for 2 h. Washing was performed 2–3 times at each subsequent step. Detection antibody was added to each well and incubated for 1 h, followed by the addition of an HRP-conjugated enzyme reagent. The plates were incubated for 30 min in the dark using TMB substrate (BD Biosciences, San Diego, CA, USA Cat #555214). The colorimetric reaction was stopped by adding 2N H_2SO_4, and absorbance was measured at 450 nm wavelength using a spectrophotometer (SpectraMax® M2e).

Quantitative reverse transcription polymerase chain reaction (qRT-qPCR): Total RNA was extracted from BMDMs using a Trizol reagent (TRIZOL, Invitrogen Cat #15596026) as per manufacturer's instructions. Trizol-extracted RNA was treated with RNase-free DNase (Promega Catalog:M610A) to remove any genomic DNA contamination, and RNA was quantitated using Nanodrop (Nanodrop™ Thermoscientific). cDNA was synthesized using m-MLV Reverse Transcriptase (Invitrogen Cat # 28025013). Quantitative gene analysis was performed using PCR master mix (2× qPCR Universal Green MasterMix Cat # qMX-Green-25 mL, Lamda Biotech). Thermal cycling was run on a real-time PCR system (Applied Biosystems 7500 QuantStudio 6 Pro) using an optimized protocol: initial denaturation at 95.0 °C for 5 min, 95.0 °C for 15 s; annealing temperature 60 °C for 1 min; melt curve from 60 °C to 95.0 °C; increment 0.15 °C for 1 s. The Ct value of target genes obtained from each sample was normalized to the housekeeping gene GAPDH, and relative gene expression was quantified using $2^{-\Delta\Delta ct}$ values. We used GAPDH as internal control due to its abundant and stable expression in different tissues. Additionally, we used unstimulated cells as controls for qPCR studies. Table 1 presents the quantitative PCR mouse target genes and associated primer sets.

Table 1. Primers used for qPCR.

Primer	Forward Sequence	Reverse Sequence
GAPDH	5′ATGACTCCACTCACGGCAAAT3′	5′GGGTCTCGCTCCTGGAAGAT3′
TNF α	5′GAACTGGCAGAAGAGGCACT3′	5′AGGGTCTGGGCCATAGAACT3′
IL6	5′GAGGATACCACTCCCAACAGACC3′	5′AAGTGCATCATCGTTGTTCATACA3′
CXCL1	5′GCTGGGATTCACCTCAAGAA3′	5′TCTCCGTTACTTGGGGACAC3′
CCL2	5′CTTCTGGGCCTGCTGTTCA3′	5′CCAGCCTACTCATTGGGATCA3′
IFN-B	5′TCAGAATGAGTGGTGGTTGC3′	5′GACCTTTCAAATGCAGTAGATTCA3′
ISG-15	5′GGCCACAGCAACATCTATGA3′	5′CGCAAATGCTTGATCACTGT3′
CXCL10	5′GCCGTCATTTTCTGCCTCAT3′	5′GCTTCCCTATGGCCCTCATT3′
OAS1	5′ATTACCTCCTTCCCGACACC3′	5′CAAACTCCACCTCCTGATGC3′
IFITM3	5′GCCCCCAACTACGAAAGA3′	5′ATTGAACAGGGACCAGACCAC3′
TLR3	5′GTCTTCTGCACGAACCTGACAG3′	5′TGGAGGTTCTCCAGTTGGACCC3′
TLR7	5′GTGATGCTGTGTGGTTTGTCTGG3′	5′CCTTTGTGTGCTCCTGGACCTA3′

Western blot assay: Total cell extracts were lysed in RIPA buffer (Cell signaling, catalog #9806) supplemented with protease inhibitor (Thermo Scientific, Cat # 1861281) post-RNA-mimic treatment (10, 30, and 60 min). Total protein concentrations were determined using a Pierce™ BCA protein assay kit (Thermofisher Scientific, Cat # 23225). An equal amount of protein was loaded for SDS-PAGE on 10% polyacrylamide gels, electro-transferred to nitrocellulose membrane (Bio-Rad 0.45 µM #1620115), and probed with primary antibody overnight at 4 °C. The primary antibodies used included anti-phosphorylated p44/42 MAPK (Cell signaling # 9101, 1:1000), anti-p44/42 MAPK (Cell signaling # 4695, 1:1000), anti-phosphorylated p38 MAPK (Cell signaling # 4511, 1:1000), anti-p38 MAPK (Cell signaling # 8690, 1:1000), anti-phosphorylated SAPK/JNK (Cell signaling # 9255, 1:1000), anti-SAPK/JNK (Cell signaling # 9252, 1:1000), anti-phosphorylated NF-kB p65 (Cell signaling # 3033, 1:1000), anti-NF-kB p65 (Cell signaling # 8242, 1:1000), and β-actin (Invitrogen # MA5-15739). The membrane was washed 3X times with TBST wash buffer and incubated with appropriate secondary antibody for 1 h, then visualized using Amersham Imager 600. The secondary antibodies used were Anti-Mouse IgG (Jackson ImmunoResearch Cat #115-035-003) and Anti-Rabbit IgG (Invitrogen # 31460). Beta-actin was used as a loading control. For densitometry, images were analyzed using Image J software Version 1.53.

Flow Cytometry: Surface and intracellular expression of TLR3 and TLR7 on BMDMs were determined by FACS analysis. A total of 1.5×10^5 cells/well were seeded on a 96-well round-bottom plate. For cell surface staining, cells were stained with PECy7 α-CD45 (Biolegend) Pacific Blue™ anti-mouse/human CD11b (Biolegend) and APC anti-mouse F4/80 (BioLegend), and incubated for 20 min at 4 °C in the dark. After incubation, cells were washed once with FACS buffer (1× PBS; 2% FBS, 0.05% NaA2), followed by centrifugation at 1200× *g* for 5 min at 4 °C. Intracellular expression of TLR3 or TLR7 was determined following fixation and permeabilization using a Cytofix/Cytoperm Kit (BD Bioscience Catalog #554655) for 20 min at 4 °C. After incubation, cells were washed with 1× perm buffer (diluted from 10× stock containing Fetal Bovine Serum (FBS) and saponin) followed by staining with Intracellular antibodies PE anti-mouse CD283 TLR3 (Biolegend) and BD Pharminogen™ PE Mouse Anti-Mouse TLR7 (CD287) (BD Biosciences). All surface and intracellular antibodies were diluted 1:200 in FACS buffer for surface staining or perm buffer for intracellular staining. After incubating with intracellular antibodies, cells were washed with FACS buffer followed by centrifugation at 1200× *g* for 5 min at 4 °C and resuspended in 200 µL of FACS buffer for FACS acquisition. Samples were acquired using BD FACS-ARIA-III™ and were analyzed using FlowJo™ software (Tree Star). Table 2 presents the antibodies used for flow cytometry with their source and catalog number.

Table 2. Antibodies used for flow cytometry.

Antibody	Detection	Source and Catalog Number
PECy7 anti-mouse CD45	CD45	Biolegend cat#103114/clone 30-F11
Pacific Blue™ anti-mouse/human CD11b	CD11b	Biolegend cat#101224/clone M1/70
APC anti-mouse F4/80	F4/80	Biolegend cat#123116/clone BM8
PE anti-mouse CD283 (TLR3)	TLR3	Biolegend cat#141904/clone 11F8
BD Pharminogen™ PE Mouse Anti-Mouse TLR7 (CD287)	TLR7	BD Biosciences cat#565557/clone A94B10

Statistical analysis: Statistical analysis was performed using GraphPad Prism Version 10.0.3 (GraphPad Software Inc., La Jolla, CA, USA). Results were analyzed using one-way ANOVA. The data in bar graphs are represented as mean +/− standard error of the mean (SEM). Threshold values of * $p < 0.05$, ** $p < 0.01$, *** $p < 0.001$, or **** $p < 0.0001$ were used to assess statistical significance.

3. Results

3.1. Viral ssRNA and dsRNA Mimics Induce Differential Inflammatory and Antiviral Responses

Excessive inflammation caused by RNA viruses is a key determinant of poor clinical outcomes [47,48]. However, the key virus and host factors driving RNA virus-induced lethal inflammation and severe disease are poorly described. Since both viral ssRNA and dsRNA are released extracellularly upon lytic infection [19,37] and are detected by the immune sensors on the sentinel or circulating myeloid cells, we evaluated whether ssRNA and dsRNA and their respective cell-surface/endosomal TLRs elicit differential inflammatory cytokine and chemokine responses. For these studies, murine BMDMs were treated with ssRNA mimic (R848) and dsRNA mimic (Poly I:C). Cells collected in Trizol at 8 h post stimulation or cell supernatants collected at 8 and 24 h poststimulation were used to assess the mRNA and protein levels, respectively, of inflammatory cytokines and chemokines. Our results show a significant increase in mRNA levels of inflammatory cytokines and chemokines in R848-treated BMDMs compared to Poly I:C-treated cells (Figure 1A). Further examination of the protein levels of representative inflammatory cytokines (TNF- α and IL-6) also revealed markedly higher levels of these inflammatory mediators in R848-treated cells compared to Poly I:C-stimulated cultures (Figure 1B). Next, we examined the effect of R848 and Poly I:C on antiviral IFN-I and ISG responses. Cells in trizol and cell supernatants collected at 8 and 24 h post stimulation were used to measure mRNA or protein levels of IFNs and ISGs. As shown in Figure 1C,D, we observed marginal to no IFN and ISG response in R848-stimulated macrophages compared to unstimulated cells, whereas Poly I:C treatment induced a robust increase in IFN and ISG levels. Poly I:C activates both TLR3-TRIF and MDA5-MAVS in fibroblasts [49]. Therefore, to confirm Poly I:C-induced antiviral and inflammatory response in macrophages is mediated by TLR3-TRIF signaling, we stimulated wild-type and TRIF−/− cells with Poly I:C. Our results showed a complete loss of antiviral and inflammatory cytokine production in Poly I:C-treated TRIF−/− cells compared to wild-type cells (Figure 2A), suggesting that Poly I:C-induced immune response in macrophages is dependent on TLR3-TRIF activity. We also confirmed that R848-mediated cytokine/chemokine response is Myd88-dependent (Figure 2B). These results collectively demonstrate that extracellularly derived viral ssRNA mimic induces significantly elevated levels of inflammatory cytokine/chemokines compared to dsRNA mimic, whereas dsRNA is a more potent inducer of IFN and ISG responses than ssRNA in mouse macrophages.

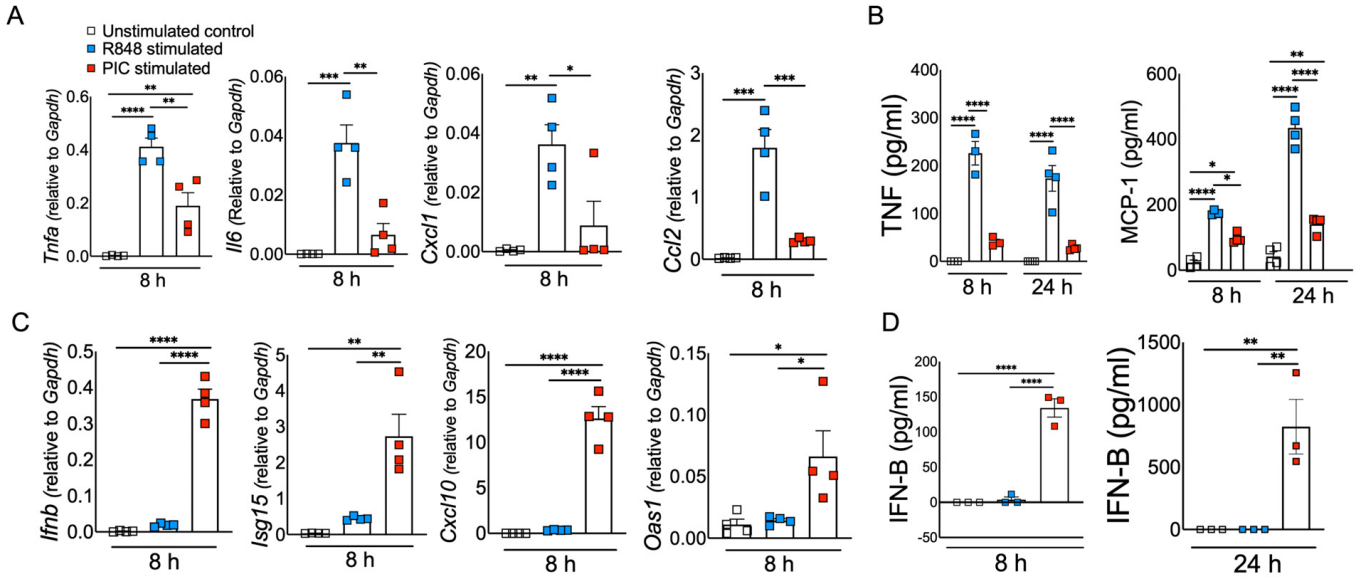

Figure 1. ssRNA/TLR7 stimulation induces robust inflammatory cytokine/chemokine responses, whereas dsRNA mimics are potent inducers of antiviral IFN and ISG responses. Murine BMDMs were stimulated with viral RNA mimics, namely R848 (ssRNA mimic) and poly I:C (dsRNA mimic), each with 10 ug/mL. mRNA (**A**) and protein levels (**B**) of inflammatory cytokines and chemokines and mRNA (**C**) and protein levels (**D**) of interferons and ISGs were assessed 8 and 24 h after stimulation, respectively. Data are representative of three independent experiments. Statistical significance was determined using one-way ANOVA with * $p < 0.05$, ** $p < 0.01$, *** $p < 0.001$, and **** $p < 0.0001$.

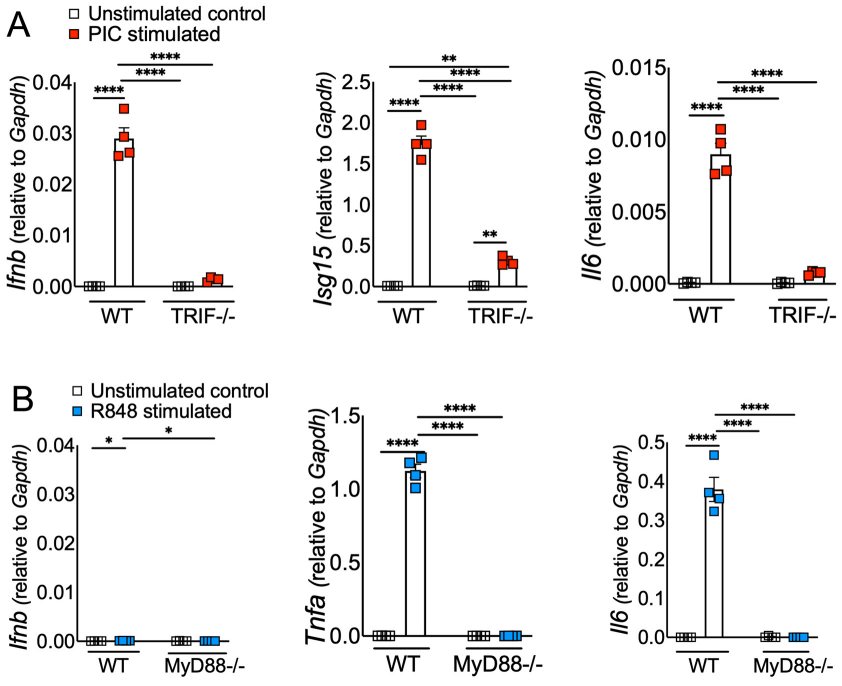

Figure 2. ssRNA/TLR7 elicits inflammatory cytokine/chemokine responses via MyD88, whereas dsRNA mimics elicit IFN and ISG response via TRIF signaling. WT and TRIF-/- BMDMs (**A**) and WT and MyD88-/- BMDMs (**B**) were stimulated with viral RNA mimics, namely poly I:C (dsRNA mimic) and R848 (ssRNA mimic), each with 10 ug/mL, respectively. mRNA levels of interferons and inflammatory cytokines were assessed 8 h post stimulation. Data are representative of three independent experiments. Statistical significance was determined using one-way ANOVA with * $p < 0.05$, ** $p < 0.01$, and **** $p < 0.0001$.

3.2. Macrophages Express Differential Levels of Cell-Surface and Endosomal TLR3 and TLR7

Macrophages express high levels of TLRs, and recognition of viral PAMPs by these TLRs plays a crucial role in antiviral and inflammatory response [50,51]. Extracellularly derived viral dsRNA and ssRNA are primarily recognized by cell-surface/endosomal TLR3 and TLR7, respectively [27,52]. Since we observed differential antiviral and inflammatory cytokine response following TLR3 and TLR7 agonist administration, our initial question was whether TLR expression altered by macrophages contributes to differential antiviral and inflammatory cytokine production. To test this possibility, we examined cell-surface and endosomal TLR3 and TLR7 expression in murine BMDMs. As shown in Figure 3A,B, flow cytometry data showed that the percentage of macrophages expressing cell-surface and endosomal TLR7 was significantly higher than for TLR3 expression. Additionally, we found a 5–10-fold increase in mean fluorescence intensity (MFI, i.e., number of molecules expressed per cell) of TLR7 expression in endosomes than on the cell surface (Figure 3C). Although our flow cytometry results using same fluorochrome-labelled anti-TLR3 and anti-TLR7 antibodies showed high TLR7 expression in MBDMs, it is possible this difference is due to altered affinity/avidity of the antibodies used in our studies. To exclude this possibility, we measured the mRNA levels of TLR3 and TLR7 in naïve BMDMs. Consistent with FACS results, we observed high mRNA levels of TLR7 compared to TLR3 (Figure 3D). These results show a significantly higher expression of TLR7 in macrophages compared to TLR3, which may contribute to the differential inflammatory and antiviral immune response observed following ssRNA mimic/TLR7 agonist treatment compared to the dsRNA mimic/TLR3 agonist administration.

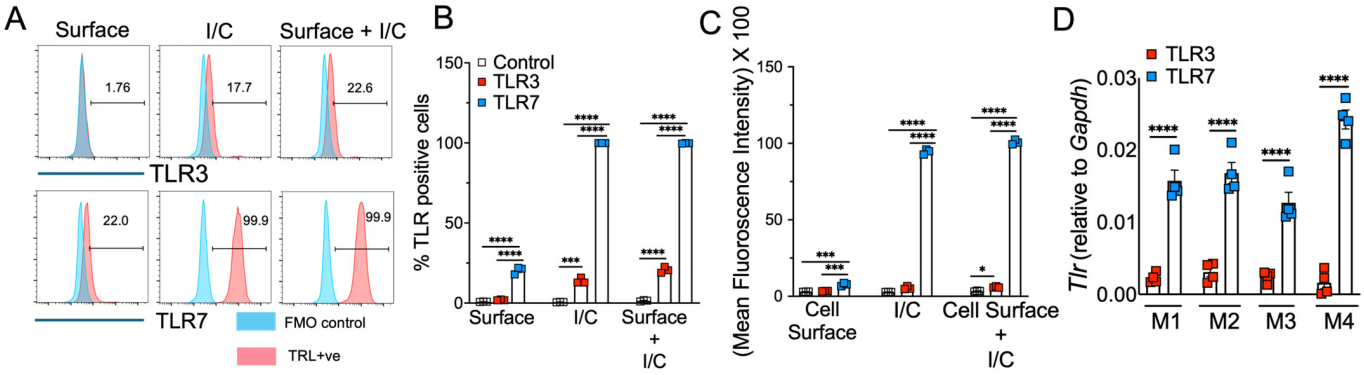

Figure 3. TLR3 and TLR7 expression in mouse bone marrow macrophages. Expression of cell-surface, intracellular, and mRNA levels of TLR3 and TLR7 in naïve mouse bone marrow macrophages was analyzed by flow cytometry (FACS) (**A**–**C**) and qRT-qPCR (**D**) using standard protocols. Scatter plot graphs show the percentage and mean fluorescent intensity of TLR3- and TLR7-positive cells (**B**,**C**) and TLR3 and TL7 mRNA expression in naïve BMDMs (**D**). Data represent 3–4 technical replicates each from 3–4 biological replicates. Statistical significance was determined using one-way ANOVA with * $p < 0.05$, *** $p < 0.001$ and **** $p < 0.0001$.

3.3. R848 and Poly I:C Induce Differential MAPK and NF-kB Activation in Macrophages

Our results showed differential inflammatory cytokine response in Poly I:C- and R848-treated cells (Figure 1), which was in agreement with cell-surface and endosomal TLR3/7 expression (Figure 3). However, these results fail to show whether or not such differential TLR3/7 expression corresponds with altered downstream signaling. TLR7 facilitates MyD88-TRAF6, and TLR3 utilizes TRIF-TRAF6 adapters to induce the NF-kB/MAPK-mediated inflammatory cytokine response [53,54]. Therefore, to determine the mechanistic basis for R848/TLR7- and Poly I:C/TLR3-induced differential inflammatory cytokine response, we stimulated primary mouse BMDMs with these viral ssRNA and dsRNA mimics. The cell lysates collected at 10, 30, and 60 min were analyzed for total and phospho-levels of MAPKs and NF-kB using Western blot assay. As shown in

Figure 4A, we observed a significant increase in phosphorylation of MAPK (p-ERK, p-P38, and p-JNK) and NF-kB (p-P65) pathways in R848-stimulated macrophages as early as 10 min post stimulation, which persisted for up to 30 min post stimulation. In contrast, we observed a delay in Poly I:C-induced phosphorylation of these pathways, with robust MAPK/NF-kB activity observed at 60 min post stimulation (Figure 4A,B). These results indicate that R848–TLR7 signaling promotes early activation of MAPK and NF-kB pathways, whereas Poly I:C-TLR3 signaling is a delayed and muted activator of these downstream pathways.

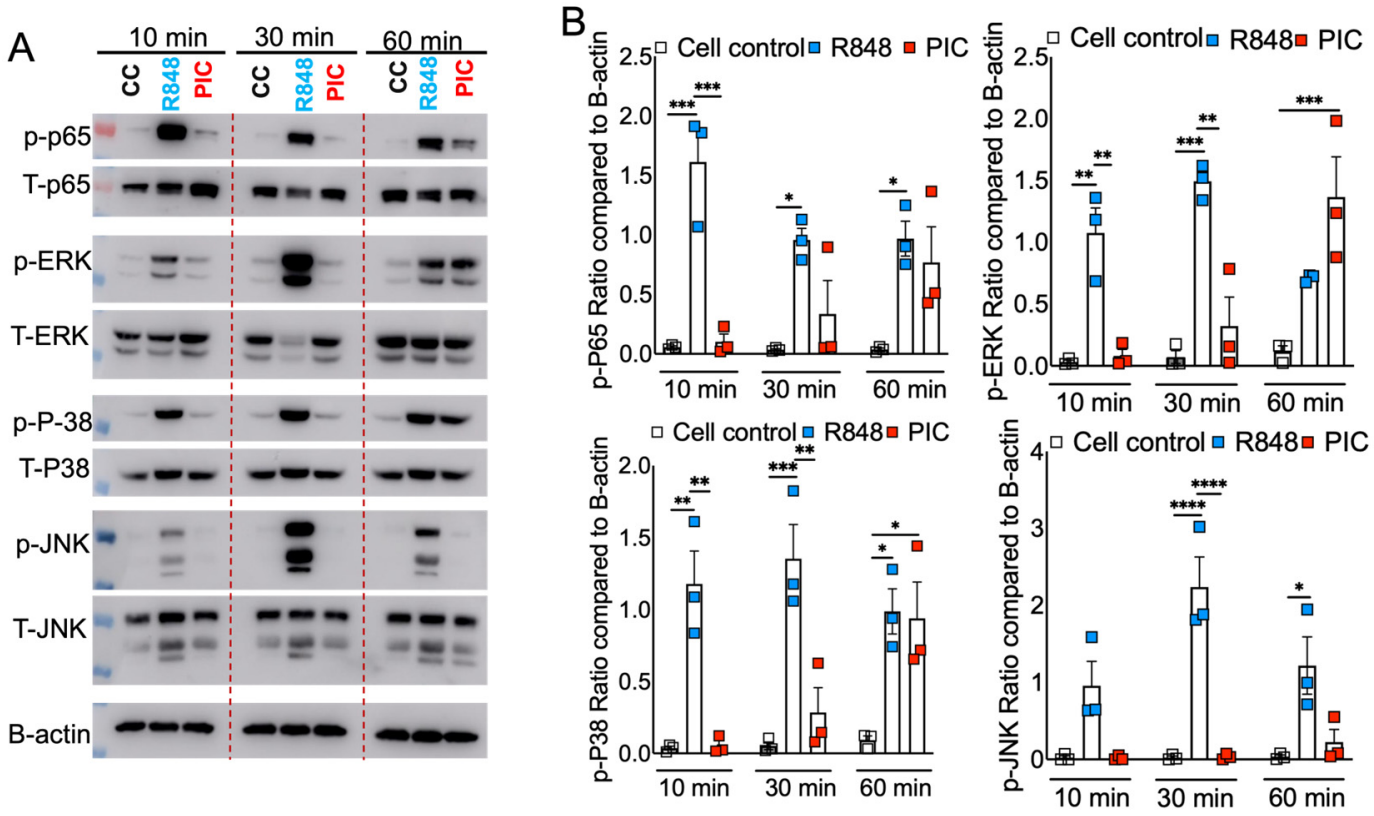

Figure 4. RNA mimic stimulation induced differential phosphorylation of MAPK and NF-kB signaling. Murine bone marrow macrophages were treated with ssRNA mimic (R848) and dsRNA mimic (PIC), each with 10 ug/mL, for 10, 30, and 60 min. Cell lysates were collected, and Western blot was performed using mAbs against phosphorylated MAPK (p-ERK1/2 (phospho-ERK1/2), p-P38 (phospho-P38), and p-JNK (phospho-JNK) and NF-kB (p-P65 (phospho-P65)). and their total proteins were denoted as T-ERK, T-P38, T-JNK, and T-P65, respectively (**A**), and relative quantification of protein levels were measured by densitometry analysis (**B**). Data are representative of three independent experiments (**A**) or pooled from three independent experiments (**B**). Statistical significance was determined using one-way ANOVA with * $p < 0.05$, ** $p < 0.01$, *** $p < 0.001$ and **** $p < 0.0001$.

3.4. Blocking ERK1/2 Reduces Inflammation and Improves IFN in Viral RNA Mimic-Treated Cells

Our results thus far illustrate that dysregulated immunity in ssRNA mimic-treated cells corresponds with high TLR7 expression and TLR7-induced robust MAPK/NF-kB activation (Figures 1–4). To further demonstrate that TLR7-induced robust MAPK and NF-kB activity promotes excessive inflammation, we blocked MAPK and NF-kB signaling using well-established inhibitors for each pathway. First, we evaluated the ability of MAPK and NF-kB inhibitors to block pathway-specific activity. As shown in Figure 5A, TLR-stimulated BMDMs pre-treated with specific inhibitors of ERK1/2 (Trametinib), p38 (Losmapimod), JNK (JNK inhibitor I), and NF-kB (BAY11-7082) showed reduced phosphorylation of respective proteins compared to untreated cells. Next, cell supernatants collected from control

and pathway-specific inhibitor-treated BMDMs stimulated with R848 or Poly I:C (10 g/mL each) were examined for TNF, MCP-1, and IFN-β levels. As expected, blocking p-ERK1/2, p-NF-kB, and p-JNK activity all reduced inflammatory cytokine and chemokine (except for JNK inhibition) production (Figure 5B). However, to our surprise, p-p38 inhibition enhanced inflammatory cytokines/chemokine levels in BMDM cultures (Figure 5B). Interestingly, p-ERK1/2 inhibition improved type IFN-I levels (Figure 5C) in both R848- and Poly I:C-treated cells, which corresponded with enhanced ISG levels at both 8 and 24 h in R848-treated cells and at 24 h in Poly I:C-treated cells (Figure 6A,B). Conversely, blocking NF-kB suppressed IFN-β levels, whereas p38 and JNK inhibition had minimal impact on IFN-I response (Figure 5C). Collectively, these results establish that (a) TLR7-induced robust MAPK/NF-kB activation promotes excessive inflammation, and (b) ERK1/2 signaling promotes inflammatory cytokine/chemokine levels while suppressing viral RNA mimics-induced IFN-I and ISG responses.

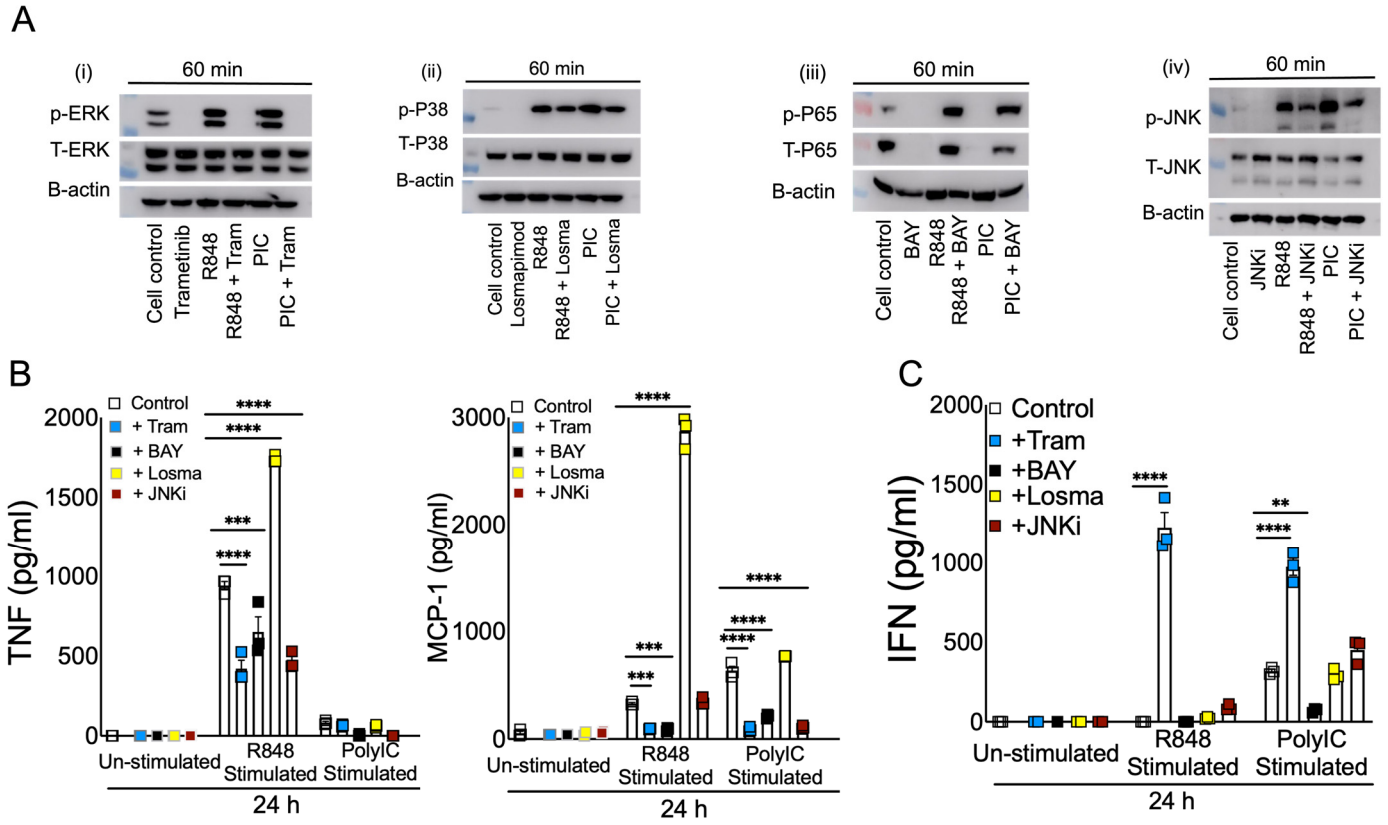

Figure 5. Effect of blocking MAPK and NF-kB signaling in viral RNA mimic-induced inflammatory and antiviral cytokine response. Murine BMDMs were treated with specific inhibitors (5 μM) of ERK1/2 (**i**), p38 (**ii**), NF-kB (**iii**), and JNK (**iv**) pathways for 2 h followed by stimulation with R848 and or Poly I:C, each with 5–10 ug/mL. Western blot showing the inhibitory effect of Trametinib, Losmapimod, BAY, and JNKi on phospho-ERK (p-ERK), phospho-P38 (p-P38), phospho-P65(p-P65), and phospho-JNK(p-JNK), respectively, and their total proteins, denoted as T-ERK, T-P38, T-P65, and T-JNK, respectively. (**A**) Protein levels of cytokines and interferons (**B**,**C**) were assessed at 8 and 24 h post stimulation. Data are representative of 2–3 independent experiments (**B**,**C**). Statistical significance was determined using one-way ANOVA with ** $p < 0.01$, *** $p < 0.001$ and **** $p < 0.0001$.

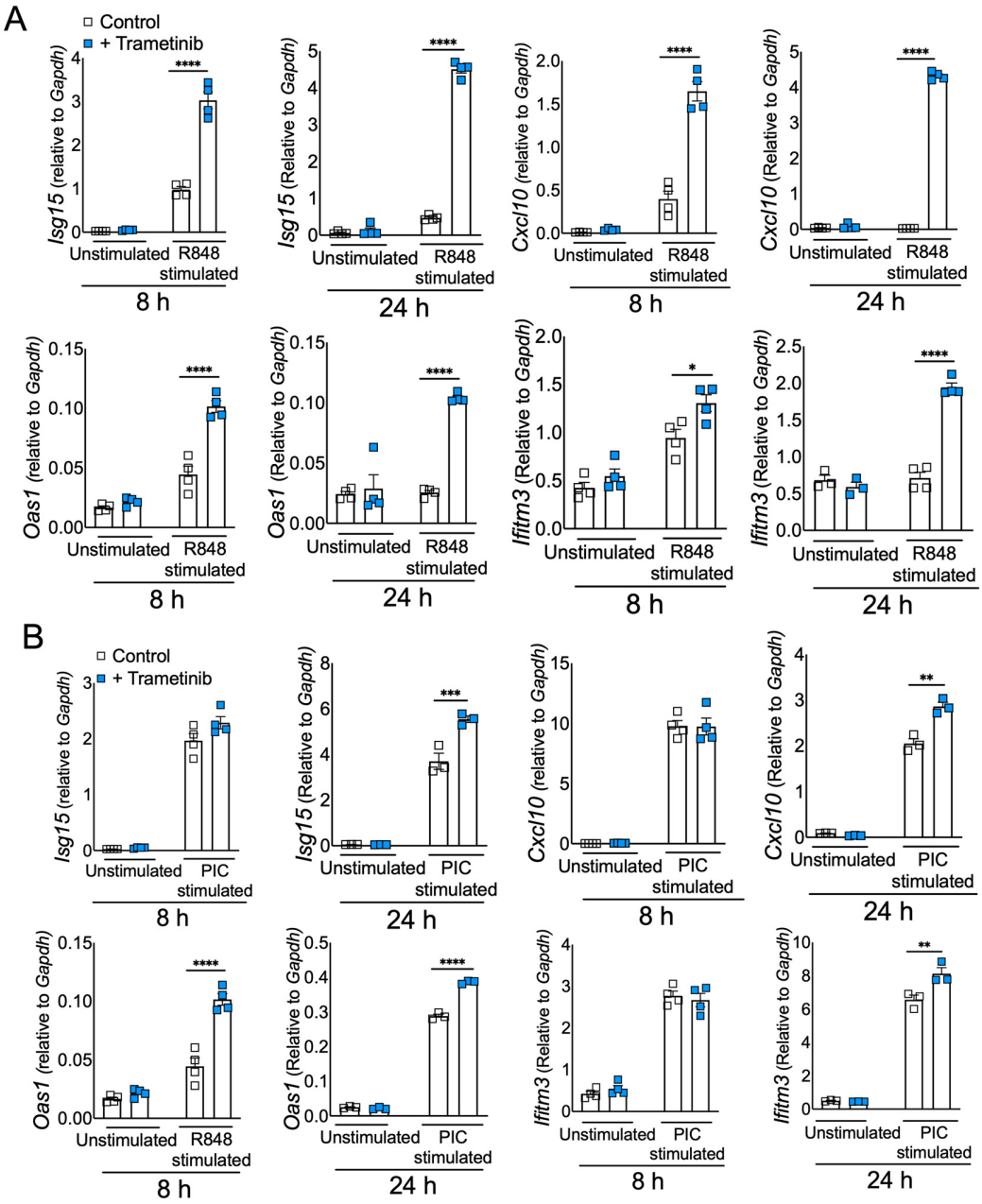

Figure 6. Inhibiting ERK1/2 signaling enhances antiviral interferon response in viral RNA mimic-treated cells. Murine BMDMs were treated with Trametinib (5 μM) inhibitor of ERK1/2 pathway for 2 h, followed by stimulation with R848 and or Poly I:C, each with 5–10 ug/mL. mRNA levels of ISGs with R848 and PIC stimulations, respectively, with and without Trametinib (**A**,**B**) were assessed at 8 and 24 h post stimulation. Data are representative of 2–3 independent experiments. Statistical significance was determined using one-way ANOVA with * $p < 0.05$, ** $p < 0.01$, *** $p < 0.001$ and **** $p < 0.0001$.

4. Discussion

Emerging and re-emerging RNA viruses such as influenza, coronaviruses, Ebola virus, hantavirus, and Nipah virus cause acute and often fatal illness [55,56]. The RNA virus-induced severe disease is caused by excessive inflammatory and impaired or delayed antiviral IFN/ISG responses [13,14]. Additionally, ssRNA-induced severe inflammation is associated with excessive monocyte/macrophage accumulation [57–60]. However, the basis for RNA virus-induced lethal inflammation and the host factors that suppress antiviral IFN/ISG responses need to be well defined for mitigating severe diseases caused by RNA

viruses. Viral RNAs are critical orchestrators of antiviral and inflammatory responses, and monocyte/macrophages are a key source of inflammatory mediators and IFNs [12,37,61,62]. Therefore, in this study, using RNA mimics, we examined the effects of viral ssRNA and dsRNA in eliciting macrophage-induced inflammatory and antiviral responses. Our results illustrate that viral ssRNA mimics induce a robust inflammatory but a poor IFN response, whereas dsRNA mimics elicited a strong IFN and a relatively weak inflammatory cytokine response. We further demonstrated that viral ssRNA and dsRNA mimic-mediated differential immune response is likely driven by the high cell-surface and endosomal TLR7 expression as opposed to low TLR3 expression. Excessive inflammatory cytokine response and high cell-surface/endosomal TLR expression are associated with early and robust NF-kB and MAPK activation in TLR7 compared to TLR3 agonist-treated cells. Finally, we demonstrated that blocking NF-kB and MAPK sub-pathways reduces viral RNA mimic-induced inflammatory cytokine production, while only ERK1/2 inhibition significantly increased IFN/ISG responses. Our results, albeit using viral RNA mimics, collectively explain the basis for the dysregulated immunity caused by RNA viruses.

The differential roles of TLR7 and TLR3 in inducing inflammatory and antiviral cytokines have been previously described [27,63,64]. However, most of these studies have examined either TLR7 and TLR3 agonist-induced inflammatory cytokine response or antiviral IFN/ISG response without defining the implications of these results in RNA virus-induced dysregulated immunity. The majority of emerging RNA viruses consist of the ssRNA genome that makes intermediate dsRNA during replication [65]. Therefore, we believe that it is critical to clearly define the role of viral ssRNA and dsRNA in eliciting inflammatory cytokine/chemokine and antiviral immune responses. In this study, we used well-described viral ssRNA and dsRNA mimics to examine both mRNA and protein levels of inflammatory cytokines and IFN/ISGs at both early and late times to comprehensively describe the role of viral RNAs in monocyte/macrophage-mediated immune response. Although the use of viral ssRNA and dsRNA mimics instead of authentic viral ssRNA or dsRNA is a limitation in our study, we strongly believe that our results lay a foundation for a careful examination of virion-purified, in vitro-synthesized, or in vivo-generated viral ssRNA and dsRNA in causing dysregulated immunity and severe disease.

In addition to detailed examination of viral ssRNA and dsRNA mimic-induced inflammatory and antiviral immunity, our study provides a potential mechanistic explanation for differential immune response induced by viral RNA mimics. It illustrates that high cell-surface and endosomal TLR7 expression compared to TLR3 levels are associated with R848-induced robust inflammatory cytokine production. Conversely, cell-surface/ endosomal TLR7 levels did not associate with IFN response, as shown by low IFN/ISG levels in R848-treated cells compared to Poly I:C-treated macrophages. These results suggest TLR7/Myd88 signaling is a weak IFN-I/ISG inducer compared to TLR3/TRIF activity. An additional explanation for Poly I:C-induced high IFN/ISG levels is that the dsRNA is escorted into the cytosol and sensed by MDA5 [66,67]. Since inflammatory monocyte/macrophages are the key cell types associated with elevated cytokine response during SARS infection [57–59], we used macrophages for our study. Yet, data are lacking for other cell types, especially pDCs, where there is robust IFN response during viral infection,. However, our results show that at least in macrophages, Poly I:C-induced IFN/ISG response is mediated via the TLR3-TRIF pathway. We further show that high TLR7 and inflammatory cytokine levels correspond with robust NF-kB and MAPK (p38, ERK1/2, and JNK) activity as early as 10 min post R848/TLR7 stimulation compared to Poly I:C treatment. Additionally, TLR7 induced robust activation of NF-kB and MAPK at both 30 and 60 min post stimulation. These results collectively suggest that the timing and strength of NF-kB and MAPK activity dictate the level of inflammatory cytokine and chemokine production in viral RNA mimic-treated cells. Although previous studies have examined the role of either NF-kB or MAPK activity in viral RNA mimic-treated and RNA virus-infected cells, our work comprehensively examines multiple key signaling pathways

at several time points, providing critical and detailed insight into the role played by these pathways in viral RNA-induced inflammation and antiviral response [68,69].

This study shows the robust activation of multiple pathways in ssRNA mimic-treated cells and identifies the impact of blocking these pathways in mitigating excessive inflammation. Significant reduction in inflammatory cytokine/chemokine levels in NF-kB-, ERK1/2-, and JNK-inhibitor-treated cells highlights the importance of simultaneously blocking multiple pathways to mitigate viral ssRNA-induced inflammation. Of note, in contrast to published results demonstrating the anti-inflammatory functions of FDA-approved p38-MAPK inhibitor Losmapimod, we consistently observed a significant increase in inflammatory cytokine/chemokine levels in Losmapimod-treated and TLR7-stimulated—but not Poly I:C-treated—macrophages [70,71]. These results suggest that blocking p38 likely exacerbates viral ssRNA-induced inflammation. Although it is unclear if such response is specific to Losmapimod treatment in BMDMs or is a general response to p38 inhibition in all cell types, these outcomes warrant a further investigation of immunomodulatory effect of Losmapimod, particularly during RNA virus infection. Thus, treating with Losmapimod simultaneously in both raw and differentiated macrophages might support these results. Another important finding from our study is that, unlike blocking NF-kB and JNK signaling, ERK1/2 inhibition significantly improved antiviral IFN/ISG response in ssRNA and dsRNA mimic-treated cells, emphasizing the importance of blocking ERK1/2 activity to suppress excessive inflammatory cytokines and simultaneously improve antiviral IFN/ISG response. Although corticosteroids are currently used to suppress exuberant inflammation, corticosteroid-mediated suppression of antiviral innate and adaptive immunity is a clinical concern [72,73]. Therefore, blocking ERK1/2 signaling along with NF-kB and other MAPK pathways is likely superior to provide better protection compared to the current immunomodulatory therapies.

In summary, using viral RNA mimics, our research demonstrates that ssRNA, which is abundantly produced during RNA virus infections, is potentially a key mediator of virus-induced exuberant inflammation and impaired antiviral IFN/ISG response. Mechanistically, we showed that high cell-surface and endosomal TLR7 expression drives robust NF-kB and MAPK activation, thus facilitating excessive inflammatory cytokine response. Additionally, given that ERK1/2 signaling suppresses antiviral response and promotes inflammation, blocking ERK1/2 activity is perhaps a better immunomodulatory strategy to mitigate dysregulated immunity and provide better protection.

Author Contributions: R.C. and R.S. conceptualized the study; R.S., P.M.J., R.G. and C.J.W. carried out experiments and data analysis; R.C. and R.S. wrote the manuscript; R.C., R.S., P.M.J., R.G. and C.J.W. reviewed and edited the manuscript; R.C. provided mentoring and supervised experiments, data analysis, and presentation. All authors have read and agreed to the published version of the manuscript.

Funding: We acknowledge funding support from National Institutes of Health (NIH), USA. NIH: R21AI186028-01, NIH: R01HL165423-01A1, NIH: P30GM149368-02.

Institutional Review Board Statement: This work is approved by Institutional Animal Care and Use Committee (IACUC) under the protocol number 21-05.

Informed Consent Statement: Not applicable.

Data Availability Statement: The original contributions presented in the study are included in the article, further inquiries can be directed to the corresponding author.

Acknowledgments: This work is supported in part by an institutional research fund to RC from Oklahoma State University, College of Veterinary Medicine. We also acknowledge OCRID/CoBRE Immunopathology Core for assistance in flow cytometry studies.

Conflicts of Interest: The authors declare no conflict of interest.

References

1. Abdelwhab, E.M.; Mettenleiter, T.C. Zoonotic Animal Influenza Virus and Potential Mixing Vessel Hosts. *Viruses* **2023**, *15*, 980. [CrossRef] [PubMed]
2. Woolhouse, M.E.J.; Gowtage-Sequeria, S. Host Range and Emerging and Reemerging Pathogens. *Emerg. Infect. Dis.* **2005**, *11*, 1842–1847. [CrossRef] [PubMed]
3. Taylor, L.H.; Latham, S.M.; Woolhouse, M.E. Risk factors for human disease emergence. *Philos. Trans. R. Soc. Lond. B Biol. Sci.* **2001**, *356*, 983–989. [CrossRef]
4. Ge, X.-Y.; Li, J.-L.; Yang, X.-L.; Chmura, A.A.; Zhu, G.; Epstein, J.H.; Mazet, J.K.; Hu, B.; Zhang, W.; Peng, C.; et al. Isolation and characterization of a bat SARS-like coronavirus that uses the ACE2 receptor. *Nature* **2013**, *503*, 535–538. [CrossRef]
5. Daep, C.A.; Muñoz-Jordán, J.L.; Eugenin, E.A. Flaviviruses, an expanding threat in public health: Focus on Dengue, West Nile, and Japanese encephalitis virus. *J. Neurovirol.* **2014**, *20*, 539–560. [CrossRef]
6. Martina, B.E.; Osterhaus, A.D. "Filoviruses": A real pandemic threat? *EMBO Mol. Med.* **2009**, *1*, 10–18. [CrossRef]
7. Li, W.; Shi, Z.; Yu, M.; Ren, W.; Smith, C.; Epstein, J.H.; Wang, H.; Crameri, G.; Hu, Z.; Zhang, H.; et al. Bats Are Natural Reservoirs of SARS-Like Coronaviruses. *Science* **2005**, *310*, 676–679. [CrossRef]
8. Lau, S.K.P.; Woo, P.C.Y.; Li, K.S.M.; Huang, Y.; Tsoi, H.-W.; Wong, B.H.L.; Wong, S.S.Y.; Leung, S.-Y.; Chan, K.-H.; Yuen, K.-Y. Severe acute respiratory syndrome coronavirus-like virus in Chinese horseshoe bats. *Proc. Natl. Acad. Sci. USA* **2005**, *102*, 14040–14045. [CrossRef]
9. Wang, L.F.; Eaton, B.T. Bats, Civets and the Emergence of SARS. In *Wildlife and Emerging Zoonotic Diseases: The Biology, Circumstances and Consequences of Cross-Species Transmission*; Childs, J.E., Mackenzie, J.S., Richt, J.A., Eds.; Springer: Berlin/Heidelberg, Germany, 2007; pp. 325–344. [CrossRef]
10. Plowright, R.K.; Eby, P.; Hudson, P.J.; Smith, I.L.; Westcott, D.; Bryden, W.L.; Middleton, D.; Reid, P.A.; McFarlane, R.A.; Martin, G.; et al. Ecological dynamics of emerging bat virus spillover. *Proc. R. Soc. B: Biol. Sci.* **2015**, *282*, 20142124. [CrossRef]
11. Nelemans, T.; Kikkert, M. Viral Innate Immune Evasion and the Pathogenesis of Emerging RNA Virus Infections. *Viruses* **2019**, *11*, 961. [CrossRef]
12. Channappanavar, R.; Fehr, A.R.; Vijay, R.; Mack, M.; Zhao, J.; Meyerholz, D.K.; Perlman, S. Dysregulated type I interferon and inflammatory monocyte-macrophage responses cause lethal pneumonia in SARS-CoV-infected mice. *Cell Host Microbe* **2016**, *19*, 181–193. [CrossRef] [PubMed]
13. Peiris, J.; Hui, K.P.; Yen, H.L. Host response to influenza virus: Protection versus immunopathology. *Curr. Opin. Immunol.* **2010**, *22*, 475–481. [CrossRef] [PubMed]
14. Blanco-Melo, D.; Nilsson-Payant, B.E.; Liu, W.-C.; Uhl, S.; Hoagland, D.; Møller, R.; Jordan, T.X.; Oishi, K.; Panis, M.; Sachs, D. Imbalanced host response to SARS-CoV-2 drives development of COVID-19. *Cell* **2020**, *181*, 1036–1045.e9. [CrossRef] [PubMed]
15. Werling, D.; Jungi, T.W. TOLL-like receptors linking innate and adaptive immune response. *Vet. Immunol. Immunopathol.* **2003**, *91*, 1–12. [CrossRef] [PubMed]
16. Saito, T.; Gale, M. Principles of intracellular viral recognition. *Curr. Opin. Immunol.* **2007**, *19*, 17–23. [CrossRef]
17. Zhong, B.; Tien, P.; Shu, H.B. Innate immune responses: Crosstalk of signaling and regulation of gene transcription. *Virology* **2006**, *352*, 14–21. [CrossRef]
18. Meylan, E.; Tschopp, J. Toll-Like Receptors and RNA Helicases: Two Parallel Ways to Trigger Antiviral Responses. *Mol. Cell.* **2006**, *22*, 561–569. [CrossRef]
19. Majde, J.A.; Guha-Thakurta, N.; Chen, Z.; Bredow, S.; Krueger, J.M. Spontaneous release of stable viral double-stranded RNA into the extracellular medium by influenza virus-infected MDCK epithelial cells: Implications for the viral acute phase response. *Arch. Virol.* **1998**, *143*, 2371–2380. [CrossRef]
20. Deng, X.; Hackbart, M.; Mettelman, R.C.; O'Brien, A.; Mielech, A.M.; Yi, G.; Kao, C.C.; Baker, S.C. Coronavirus nonstructural protein 15 mediates evasion of dsRNA sensors and limits apoptosis in macrophages. *Proc. Natl. Acad. Sci. USA* **2017**, *114*, E4251–E4260. [CrossRef]
21. Genoyer, E.; Wilson, J.; Ames, J.M.; Stokes, C.; Moreno, D.; Etzyon, N.; Oberst, A.; Gale, M. Exposure of negative-sense viral RNA in the cytoplasm initiates innate immunity to West Nile virus. *bioRxiv* **2024**. [CrossRef]
22. Kato, H.; Sato, S.; Yoneyama, M.; Yamamoto, M.; Uematsu, S.; Matsui, K.; Tsujimura, T.; Takeda, K.; Fujita, T.; Takeuchi, O.; et al. Cell Type-Specific Involvement of RIG-I in Antiviral Response. *Immunity* **2005**, *23*, 19–28. [CrossRef] [PubMed]
23. Andrejeva, J.; Childs, K.S.; Young, D.F.; Carlos, T.S.; Stock, N.; Goodbourn, S.; Randall, R.E. The V proteins of paramyxoviruses bind the IFN-inducible RNA helicase, mda-5, and inhibit its activation of the IFN-β promoter. *Proc. Natl. Acad. Sci. USA* **2004**, *101*, 17264–17269. [CrossRef] [PubMed]
24. Yoneyama, M.; Kikuchi, M.; Natsukawa, T.; Shinobu, N.; Imaizumi, T.; Miyagishi, M.; Taira, K.; Akira, S.; Fujita, T. The RNA helicase RIG-I has an essential function in double-stranded RNA-induced innate antiviral responses. *Nat. Immunol.* **2004**, *5*, 730–737. [CrossRef] [PubMed]
25. Kanno, A.; Tanimura, N.; Ishizaki, M.; Ohko, K.; Motoi, Y.; Onji, M.; Fukui, R.; Shimozato, T.; Yamamoto, K.; Shibata, T.; et al. Targeting cell surface TLR7 for therapeutic intervention in autoimmune diseases. *Nat. Commun.* **2015**, *6*, 6119. [CrossRef]
26. Akira, S.; Uematsu, S.; Takeuchi, O. Pathogen Recognition and Innate Immunity. *Cell* **2006**, *124*, 783–801. [CrossRef]
27. Diebold, S.S.; Kaisho, T.; Hemmi, H.; Akira, S.; Reis e Sousa, C. Innate Antiviral Responses by Means of TLR7-Mediated Recognition of Single-Stranded RNA. *Science* **2004**, *303*, 1529–1531. [CrossRef]

28. Lund, J.M.; Alexopoulou, L.; Sato, A.; Karow, M.; Adams, N.C.; Gale, N.W.; Iwasaki, A.; Flavell, R.A. Recognition of single-stranded RNA viruses by Toll-like receptor 7. *Proc. Natl. Acad. Sci. USA* **2004**, *101*, 5598–5603. [CrossRef]
29. Yamamoto, M.; Sato, S.; Mori, K.; Hoshino, K.; Takeuchi, O.; Takeda, K.; Akira, S. Cutting Edge: A Novel Toll/IL-1 Receptor Domain-Containing Adapter That Preferentially Activates the IFN-β Promoter in the Toll-Like Receptor Signaling1. *J. Immunol.* **2002**, *169*, 6668–6672. [CrossRef]
30. Martin, M.U.; Kollewe, C. Interleukin-1 receptor-associated kinase-1 (IRAK-1): A self-regulatory adapter molecule in the signaling cascade of the Toll/IL-1 receptor family. *Signal Transduct.* **2001**, *1*, 37–50. [CrossRef]
31. Morrison, D.K. MAP Kinase Pathways. *Cold Spring Harb. Perspect. Biol.* **2012**, *4*, a011254. [CrossRef]
32. Reimann, T.; Büscher, D.; Hipskind, R.A.; Krautwald, S.; Lohmann-Matthes, M.L.; Baccarini, M. Lipopolysaccharide induces activation of the Raf-1/MAP kinase pathway. A putative role for Raf-1 in the induction of the IL-1 beta and the TNF-alpha genes. *J. Immunol.* **1994**, *153*, 5740–5749. [CrossRef] [PubMed]
33. Hall, A.J.; Vos, H.L.; Bertina, R.M. Lipopolysaccharide Induction of Tissue Factor in THP-1 Cells Involves Jun Protein Phosphorylation and Nuclear Factor κB Nuclear Translocation. *J. Biol. Chem.* **1999**, *274*, 376–383. [CrossRef] [PubMed]
34. Yamamoto, M.; Sato, S.; Hemmi, H.; Hoshino, K.; Kaisho, T.; Sanjo, H.; Takeuchi, O.; Sugiyama, M.; Okabe, M.; Takeda, K.; et al. Role of Adaptor TRIF in the MyD88-Independent Toll-Like Receptor Signaling Pathway. *Science* **2003**, *301*, 640–643. [CrossRef] [PubMed]
35. Lee, J.Y.; Marshall, J.A.; Bowden, D.S. Characterization of Rubella Virus Replication Complexes Using Antibodies to Double-Stranded RNA. *Virology* **1994**, *200*, 307–312. [CrossRef]
36. Stollar, B.D.; Stollar, V. Immunofluorescent demonstration of double-stranded RNA in the cytoplasm of sindbis virus-infected cells. *Virology* **1970**, *42*, 276–280. [CrossRef]
37. Kawai, T.; Akira, S. Innate immune recognition of viral infection. *Nat. Immunol.* **2006**, *7*, 131–137. [CrossRef]
38. Gantier, M.P.; Williams, B.R.G. The response of mammalian cells to double-stranded RNA. *Cytokine Growth Factor Rev.* **2007**, *18*, 363–371. [CrossRef]
39. Griffin, D.E. Why does viral RNA sometimes persist after recovery from acute infections? *PLoS Biol.* **2022**, *20*, e3001687. [CrossRef]
40. Sow, M.S.; Etard, J.-F.; Baize, S.; Magassouba, N.; Faye, O.; Msellati, P.; Touré, A., II; Savane, I.; Barry, M.; Delaporte, E.; et al. New Evidence of Long-lasting Persistence of Ebola Virus Genetic Material in Semen of Survivors. *J. Infect. Dis.* **2016**, *214*, 1475–1476. [CrossRef]
41. Lupi, L.; Vitiello, A.; Parolin, C.; Calistri, A.; Garzino-Demo, A. The Potential Role of Viral Persistence in the Post-Acute Sequelae of SARS-CoV-2 Infection (PASC). *Pathogens* **2024**, *13*, 388. [CrossRef]
42. Chen, B.; Julg, B.; Mohandas, S.; Bradfute, S.B.; Force, R.M.P.T. Viral persistence, reactivation, and mechanisms of long COVID. *eLife* **2023**, *12*, e86015. [CrossRef] [PubMed]
43. Zuo, W.; He, D.; Liang, C.; Du, S.; Hua, Z.; Nie, Q.; Zhou, X.; Yang, M.; Tan, H.; Xu, J.; et al. The persistence of SARS-CoV-2 in tissues and its association with long COVID symptoms: A cross-sectional cohort study in China. *Lancet Infect. Dis.* **2024**, *24*, 845–855. [CrossRef] [PubMed]
44. Kumar, R.; Khandelwal, N.; Thachamvally, R.; Tripathi, B.N.; Barua, S.; Kashyap, S.K.; Maherchandani, S.; Kumar, N. Role of MAPK/MNK1 signaling in virus replication. *Virus Res.* **2018**, *253*, 48–61. [CrossRef] [PubMed]
45. Parisien, J.-P.; Lau, J.F.; Rodriguez, J.J.; Sullivan, B.M.; Moscona, A.; Parks, G.D.; Lamb, R.A.; Horvath, C.M. The V Protein of Human Parainfluenza Virus 2 Antagonizes Type I Interferon Responses by Destabilizing Signal Transducer and Activator of Transcription 2. *Virology* **2001**, *283*, 230–239. [CrossRef] [PubMed]
46. Basler, C.F.; Mikulasova, A.; Martinez-Sobrido, L.; Paragas, J.; Mühlberger, E.; Bray, M.; Klenk, H.-D.; Palese, P.; García-Sastre, A. The Ebola Virus VP35 Protein Inhibits Activation of Interferon Regulatory Factor 3. *J. Virol.* **2003**, *77*, 7945–7956. [CrossRef]
47. Liu, Q.; Zhou, Y.H.; Yang, Z.Q. The cytokine storm of severe influenza development of immunomodulatory, therapy. *Cell. Mol. Immunol.* **2016**, *13*, 3–10. [CrossRef]
48. Zhang, Y.; Li, J.; Zhan, Y.; Wu, L.; Yu, X.; Zhang, W.; Ye, L.; Xu, S.; Sun, R.; Wang, Y.; et al. Analysis of Serum Cytokines in Patients with Severe Acute Respiratory Syndrome. *Infect. Immunity* **2004**, *72*, 4410–4415. [CrossRef]
49. Karpus, O.N.; Heutinck, K.M.; Wijnker, P.J.M.; Tak, P.P.; Hamann, J. Triggering of the dsRNA Sensors TLR3, MDA5, and RIG-I Induces CD55 Expression in Synovial Fibroblasts. *PLoS ONE* **2012**, *7*, e35606. [CrossRef]
50. Billack, B. Macrophage Activation: Role of Toll-like Receptors, Nitric Oxide, and Nuclear Factor kappa B. *Am. J. Pharm. Educ.* **2006**, *70*, 102. [CrossRef]
51. West, A.P.; Koblansky, A.A.; Ghosh, S. Recognition and Signaling by Toll-Like Receptors. *Annu. Rev. Cell Dev. Biol.* **2006**, *22*, 409–437. [CrossRef]
52. Alexopoulou, L.; Holt, A.C.; Medzhitov, R.; Flavell, R.A. Recognition of double-stranded RNA and activation of NF-κB by Toll-like receptor 3. *Nature* **2001**, *413*, 732–738. [CrossRef] [PubMed]
53. Akira, S.; Takeda, K. Toll-like receptor signalling. *Nat. Rev. Immunol.* **2004**, *4*, 499–511. [CrossRef] [PubMed]
54. Sato, S.; Sugiyama, M.; Yamamoto, M.; Watanabe, Y.; Kawai, T.; Takeda, K.; Akira, S. Toll/IL-1 Receptor Domain-Containing Adaptor Inducing IFN-β (TRIF) Associates with TNF Receptor-Associated Factor 6 and TANK-Binding Kinase 1, and Activates Two Distinct Transcription Factors, NF-κB and IFN-Regulatory Factor-3, in the Toll-Like Receptor Signaling 1. *J. Immunol.* **2003**, *171*, 4304–4310. [CrossRef] [PubMed]
55. Choi, Y.K. Emerging and re-emerging fatal viral diseases. *Exp. Mol. Med.* **2021**, *53*, 711–712. [CrossRef] [PubMed]

56. Nichol, S.T.; Arikawa, J.; Kawaoka, Y. Emerging viral diseases. *Proc. Natl. Acad. Sci. USA* **2000**, *97*, 12411–12412. [CrossRef]
57. Franks, T.J.; Chong, P.Y.; Chui, P.; Galvin, J.R.; Lourens, R.M.; Reid, A.H.; Selbs, E.; Mcevoy, C.P.L.; Hayden, C.D.L.; Fukuoka, J.; et al. Lung pathology of severe acute respiratory syndrome (SARS): A study of 8 autopsy cases from Singapore. *Hum. Pathol.* **2003**, *34*, 743–748. [CrossRef]
58. Nicholls, J.M.; Poon, L.L.; Lee, K.C.; Ng, W.F.; Lai, S.T.; Leung, C.Y.; Chu, C.M.; Hui, P.K.; Mak, K.L.; Lim, W.; et al. Lung pathology of fatal severe acute respiratory syndrome. *Lancet* **2003**, *361*, 1773–1778. [CrossRef]
59. Wong, C.K.; Lam, C.W.K.; Wu, A.K.L.; Ip, W.K.; Lee, N.L.S.; Chan, I.H.S.; Lit, L.C.W.; Hui, D.S.C.; Chan, M.H.M.; Chung, S.S.C.; et al. Plasma inflammatory cytokines and chemokines in severe acute respiratory syndrome. *Clin. Exp. Immunol.* **2004**, *136*, 95–103. [CrossRef]
60. Ding, Y.; Wang, H.; Shen, H.; Li, Z.; Geng, J.; Han, H.; Cai, J.; Li, X.; Kang, W.; Weng, D.; et al. The clinical pathology of severe acute respiratory syndrome (SARS): A report from China. *J. Pathol.* **2003**, *200*, 282–289. [CrossRef]
61. Beignon, A.-S.; McKenna, K.; Skoberne, M.; Manches, O.; DaSilva, I.; Kavanagh, D.G.; Larsson, M.; Gorelick, R.J.; Lifson, J.D.; Bhardwaj, N. Endocytosis of HIV-1 activates plasmacytoid dendritic cells via Toll-like receptor–viral RNA interactions. *J. Clin. Invest* **2005**, *115*, 3265–3275. [CrossRef]
62. Channappanavar, R.; Perlman, S. Evaluation of Activation and Inflammatory Activity of Myeloid Cells During Pathogenic Human Coronavirus Infection. *MERS Coronavirus* **2019**, *2099*, 195–204. [CrossRef]
63. Doyle, S.E.; Vaidya, S.A.; O'Connell, R.; Dadgostar, H.; Dempsey, P.W.; Wu, T.-T.; Rao, G.; Sun, R.; Haberland, M.E.; Modlin, R.L.; et al. IRF3 Mediates a TLR3/TLR4-Specific Antiviral Gene Program. *Immunity* **2002**, *17*, 251–263. [CrossRef] [PubMed]
64. Oshiumi, H.; Matsumoto, M.; Funami, K.; Akazawa, T.; Seya, T. TICAM-1, an adaptor molecule that participates in Toll-like receptor 3–mediated interferon-β induction. *Nat. Immunol.* **2003**, *4*, 161–167. [CrossRef] [PubMed]
65. Ahlquist, P. Parallels among positive-strand RNA viruses, reverse-transcribing viruses and double-stranded RNA viruses. *Nat. Rev. Microbiol.* **2006**, *4*, 371–382. [CrossRef]
66. Gitlin, L.; Barchet, W.; Gilfillan, S.; Cella, M.; Beutler, B.; Flavell, R.A.; Diamond, M.S.; Colonna, M. Essential role of mda-5 in type I IFN responses to polyriboinosinic:polyribocytidylic acid and encephalomyocarditis picornavirus. *Proc. Natl. Acad. Sci. USA* **2006**, *103*, 8459–8464. [CrossRef]
67. Kato, H.; Takeuchi, O.; Sato, S.; Yoneyama, M.; Yamamoto, M.; Matsui, K.; Uematsu, S.; Jung, A.; Kawai, T.; Ishii, K.J.; et al. Differential roles of MDA5 and RIG-I helicases in the recognition of RNA viruses. *Nature* **2006**, *441*, 101–105. [CrossRef]
68. Flory, E.; Kunz, M.; Scheller, C.; Jassoy, C.; Stauber, R.; Rapp, U.R.; Ludwig, S. Influenza Virus-induced NF-κB-dependent Gene Expression Is Mediated by Overexpression of Viral Proteins and Involves Oxidative Radicals and Activation of IκB Kinase. *J. Biol. Chem.* **2000**, *275*, 8307–8314. [CrossRef]
69. de Magalhães, J.C.; Andrade, A.A.; Silva, P.N.G.; Sousa, L.P.; Ropert, C.; Ferreira, P.C.P.; Kroon, E.G.; Gazzinelli, R.T.; Bonjardim, C.A. A mitogenic signal triggered at an early stage of vaccinia virus infection: Implication of MEK/ERK and protein kinase A in virus multiplication. *J. Biol. Chem.* **2001**, *276*, 38353–38360. [CrossRef]
70. Lomas, D.A.; Lipson, D.A.; Miller, B.E.; Willits, L.; Keene, O.; Barnacle, H.; Barnes, N.C.; Tal-Singer, R. An Oral Inhibitor of p38 MAP Kinase Reduces Plasma Fibrinogen in Patients with Chronic Obstructive Pulmonary Disease. *J. Clin. Pharmacol.* **2012**, *52*, 416–424. [CrossRef]
71. Fisk, M.; Cheriyan, J.; Mohan, D.; Forman, J.; Mäki-Petäjä, K.M.; McEniery, C.M.; Fuld, J.; Rudd, J.H.F.; Hopkinson, N.S.; Lomas, D.A.; et al. The p38 mitogen activated protein kinase inhibitor losmapimod in chronic obstructive pulmonary disease patients with systemic inflammation, stratified by fibrinogen: A randomised double-blind placebo-controlled trial. *PLoS ONE* **2018**, *13*, e0194197. [CrossRef]
72. Davies, J.M.; Carroll, M.L.; Li, H.; Poh, A.M.; Kirkegard, D.; Towers, M.; Upham, J.W. Budesonide and Formoterol Reduce Early Innate Anti-Viral Immune Responses In Vitro. *PLoS ONE* **2011**, *6*, e27898. [CrossRef]
73. Thomas, B.J.; Porritt, R.A.; Hertzog, P.J.; Bardin, P.G.; Tate, M.D. Glucocorticosteroids enhance replication of respiratory viruses: Effect of adjuvant interferon. *Sci. Rep.* **2014**, *4*, 7176. [CrossRef]